Appeared in *IET Image Processing*, Vol. 10, Issue 6, pp. 429-437, June 2016

Context-Based Prediction Filtering of Impulse Noise Images

Arpad Gellert *, Remus Brad

Computer Science and Electrical Engineering Department, Lucian Blaga University of Sibiu, Emil Cioran Street, No. 4, 550025 Sibiu, Romania
***** E-mail: arpad.gellert@ulbsibiu.ro

Abstract: The paper presents a new image denoising method for impulse noise in grayscale images using a context-based prediction scheme. The algorithm replaces the noisy pixel with the value occurring with the highest frequency, in the same context as the replaceable pixel. Since it is a context-based technique, it preserves the details in the filtered images better than other methods. In the aim of validation, we have compared the proposed method with several existing denoising methods, many of them being outperformed by the proposed filter.

Keywords: Context-based prediction, Markov chain, denoising, filtering, impulse noise

1. Introduction

Digital images are often affected by different types of noise, due to various sources of interferences. There are two main noise categories: Gaussian and impulse. The first mentioned type is a statistical noise, whose values are Gaussian-distributed. On the other hand, impulse noise is independent, uncorrelated with the image pixels and randomly distributed. Digital images can be degraded by impulse noise during sensors acquisition or transmission through a faulty communication channel. Salt-and-pepper is a typical impulse noise composed of minimum and maximum valued pixels within the affected image. The main objective of salt-and-pepper denoising methods is preservation of unaffected pixels while restoring the missing information.

In this paper we are proposing a novel technique to reduce salt-and-pepper noise from grayscale images using context-based prediction filtering (CBPF). The basic idea was to replace the pixel affected by noise with the pixel which occurred with the highest frequency in the same context as the replaceable pixel. Therefore, we search for the context in the vicinity of the noisy pixel. The frequencies of pixels occurring in a certain context have been determined like in a Markov chain. Since our method is using context information, it is a good candidate to reconstruct details in the images affected by noise. We have compared our technique with other existing denoising methods in terms of mean square error (MSE) and peak signal-to-noise ratio (PSNR), using the Boat, Cameraman and Airplane test images. In view of the comparisons, we have predetermined the optimal CBPF configuration and also choose the best parameters of the mentioned filters. The experimental results showed that the CBPF significantly outperforms many of the salt-and-pepper noise filters existing in the literature.

The paper is organized as follows. Section 2 reviews the state-of-the-art in denoising techniques, while Section 3 introduces the proposed CBPF. Section 4 describes the experimental methodology and the obtained results are presented in Section 5. Finally, Section 6 summarizes the relevant contributions and presents some further work directions.

2. Related Work in Impulse Noise Filtering

Impulse noise filtering techniques can be classified in three main categories: statistical based, fuzzy and neural network based and hybrid, employing multi-stage filtering [1].

One of the most employed impulse noise removal methods is the median filter, efficient only for low noise densities. Thus, during the last decade several improved median based filters have been developed, with better performance on high noise levels. Many improvements focused on replacing the noisy pixel based on non-noisy pixel values. In [2], the authors proposed a method to overcome the shortcomings faced by the classical median filter at high noise densities, by considering only those pixels that are informative in the neighborhood. A filter employing two stages was proposed in [3]; in the first stage, the noisy pixel is detected, while in the second stage noisy pixels are replaced by the mean value of a 2×2 area noise-free pixels. In [4], the authors suggests a decision based algorithm which uses a 3×3 window for image denoising applied selectively for 0 and 255 pixel values. At high noise densities the median value is noisy, therefore in such cases, neighboring pixels are used to replace the noisy pixels. A modified decision based unsymmetrical median filter is proposed in [5], replacing the noisy pixel by the trimmed median value of the non-noisy pixels. When all the pixel values are 0 and 255, the noisy pixel is replaced by the mean value of the entire window. In [6] the authors recommend a modified directional-weighted-median filter to reconstruct images corrupted by salt-and-pepper noise. If the central pixel of a certain window is classified as noisy, it is replaced by a weighted median value on an optimum direction. Hamza et al. presents in [7] another median-based filter obtained by relaxing the order statistic for pixel substitution. Noise attenuation properties as well as edge and line preservation are statistically analyzed. The trade-off between noise elimination and detail preservation is also analyzed.

In [8] the progressive switching median filter is presented. The method uses an impulse detection algorithm before filtering, and thus, only a proportion of the pixels are filtered. Both the impulse detection and the noise filtering steps are progressively applied through several iterations. The results are showing an enhancement over traditional median filters, being particularly effective for highly corrupted images. Wang et al. presents in [9] a modified switching median filter, employing a two-phase denoising method. In the first phase, the adaptive vector median filter detection [10] identifies pixels likely to have been corrupted by salt-and-pepper noise. In the second phase, the noisy candidates are evaluated by using four one-dimensional Laplacian operators, which allows edge preserving. The proposed approach can effectively preserve thin lines, fine details and edges. A soft-switching median filter for impulse noise removal was presented in [11], while Jassim [12] is proposing a Kriging interpolation filter to reduce salt and pepper noise from grayscale images. First, a sequential search is performed using $k \times k$ window size to determine non-noisy pixels. The non-noisy pixels are then passed to the Kriging interpolation method to predict their absent neighbor pixels detected in the first phase as being noisy. The experimental results are showing that the Kriging interpolation filter can achieve noise reduction without damaging edges and details.

In [13], the authors present a two-stage noise adaptive fuzzy switching median filter for salt and pepper noise removal. The first stage uses a histogram of the corrupted image to identify the noisy pixels, while in the second stage detected pixels are filtered, leaving unprocessed the noise-free pixels. Fuzzy reasoning is employed to handle uncertainty introduced by noise, present in the extracted local information. Their simulation results show that the presented method outperforms some of the existing salt-and-pepper noise filters. In [14] Lin identifies impulse noise with Support Vector Machine and removes it with a fuzzy filter. Some authors are using neural networks [15], [16], [17], [18], [19], [20], [21] to filter images affected by impulse noise. Nair and Shankar [22] make use of a neural network to

identify impulse noise in corrupted images and a modified median filter to remove the detected noise. The authors of [23] present another hybrid technique implying a neural network in the detection stage and a switching filter in the removal stage.

A universal noise removal algorithm [24], working on both Gaussian and impulse noise, is introducing the spatial gradient into the Gaussian filtering framework for Gaussian noise removal and integrate their directional absolute relative differences statistic for impulse noise removal and combine them into a hybrid noise filter. Another two-stage filter which removes mixed impulse and Gaussian noise is proposed in [25].

In contrast with the above presented methods, our proposed filter is context-based and therefore it can better preserve and reconstruct details in images affected by impulse noise.

In the last years, context-based noise filters have been also proposed. Buades et al. presented in [26] the non local means denoising algorithm. The estimated value of a pixel is computed as a weighted average of all the pixels in the image, whose weights depend on the similarity between the pixels. Thus, the pixels with a similar gray level neighborhood to the replaceable pixel have larger weights in the average. In fact, this averaging approach represents the main difference between the non local means algorithm and Markov chains. In our method, the noisy pixel is replaced, instead of an average, with the most frequent pixel which occurred in similar neighborhoods. In [27], Estrada et al. proposed a stochastic image denoising method which is based on random walks over arbitrary neighborhoods of a given pixel. They sample a subset of random walks starting from a given pixel and use the probabilities of travelling between pairs of pixels as weights to combine them into the noise-free pixel. The size and shape of each distinct neighborhood are determined by the configuration and similarity of nearby pixels. In contrast, in our method we considered a neighborhood with fixed size and shape and we use it as a whole to search similar neighborhoods. Another important difference is that we replace a noisy pixel with the most frequent pixel occurring in similar neighborhoods. Wong et al. proposed another stochastic image denoising method in [28], which is based on Markov-Chain Monte Carlo sampling.

3. Description of the Proposed Context-Based Prediction Filtering

Context-based prediction can be used to determine the probability of a value, as the frequency of its occurrence in a certain context and, thus, it has been successfully applied as statistical model in several computer science areas like computational biology [29], web mining [30], ubiquitous computing [31], information retrieval [32], speech recognition [33] and even in computer architecture [34]. Similar to a Markov process, it consists in a set of N distinct states $S = \{S_1, S_2, ..., S_N\}$ [35]. In the first order model with N states, the current state depends only on the previous state:

$$P[q_t = S_j | q_{t-1} = S_i,\ q_{t-2} = S_k,\ ...] = P[q_t = S_j | q_{t-1} = S_i] \quad (1)$$

where q_t is the state at time t, the set of transition probabilities between the states S_i and S_j is $A = \{a_{ij}\}$, having $a_{ij} = P[q_t = S_j | q_{t-1} = S_i]$, $1 \le i,\ j \le N$, $a_{ij} \ge 0$ and $\sum_{j=1}^{N} a_{ij} = 1$.

Generalizing, in an order R model, the current state depends on R previous states [36]:

$$P[q_t = S_j | q_{t-1} = S_i,\ q_{t-2} = S_k,\ ...] = P[q_t = S_j | q_{t-1} = S_i,\ ...,\ q_{t-R} = S_r] \quad (2)$$

We can also express the order *R* model in a simpler form:

$$P[q_t | q_{t-1},\ q_{t-2},\ ...] = P[q_t | q_{t-1},\ ...,\ q_{t-R}] \quad (3)$$

The full probabilistic description requires to specify the current state and all the predecessor states [35], meaning that the current state in a sequence depends on all the previous states.

In the present work, we are proposing the reconstruction of grayscale images affected by impulse noise using context-based information in a similar way as in a Markov chain implementation. In Markov chains, the next state is determined based on the transition probabilities from the current context. Therefore, we have adapted the classical Markov model presented in (3), whose values are from a 1D sequence, to work with the values of a 2D area. In our application, the probability of a pixel value is determined as the frequency of its occurrence in the same or similar contexts. Thus, the noisy pixel represents the next state which must be predicted, the surrounding pixels represent the context, whereas the search area encodes the previous states through its pixel values. In the case of grayscale images, the states consist of pixel values ranging between 0 and 255. Thus, we adjusted the order *R* model as follows:

$$\begin{aligned} &P[q_{x,y} | q_{i,j}, i = 0,...,W-1,\ j = 0,...,H-1, without\ (i = x\ and\ \ j = y)] = \\ &= P\left[q_{x,y} \middle| q_{x+i,y+j},\ i, j = -\frac{CS}{2},...,\frac{CS}{2},\ 0 \le x+i < W,\ 0 \le y+j < H, without\ i = j = 0 \right] \end{aligned} \quad (4)$$

where *CS* is the context size expressed as the number of pixels from one side of the context square, *W* and *H* are the width and height of the image, respectively. Since the context is surrounding one pixel, its size can have only odd values. The pixel value $q_{x,y}$ depends on the pixel values from the surrounding context, excepting its own value. Thus, the order of the CBPF will be $R=CS^2-1$ and the context consists in *R* pixel values. The probability of a certain pixel value in a given context is determined as the frequency of that pixel value in the considered context occurring within the image.

Equation (4) implies searching the contexts in the entire image, which leads to a major disadvantage from the timing point of view. Therefore, we limit the search area, based on the search radius *SR*, as follows:

$$\begin{aligned} &P[q_{x,y} | q_{x+i,y+j}, i, j = -SR,...,SR,\ 0 \le x+i < W,\ 0 \le y+j < H, without\ i = j = 0] = \\ &= P\left[q_{x,y} \middle| q_{x+i,y+j},\ i, j = -\frac{CS}{2},...,\frac{CS}{2},\ 0 \le x+i < W,\ 0 \le y+j < H, without\ i = j = 0 \right] \end{aligned} \quad (5)$$

Obviously, we have adjusted the *SR* on the margins to keep it within the image and have considered noisy pixels having values of 0 or 255, as in [4]. When we have determined that a pixel is noisy (*N*), we have taken the context *C* of that pixel consisting in *R* pixels from the

neighborhood, and searched for that context in a larger area, with size defined by *SR*, as it is illustrated in Figure 1. The noise-free pixel value occurred in that context with the highest frequency will replace the noisy pixel value *N*.

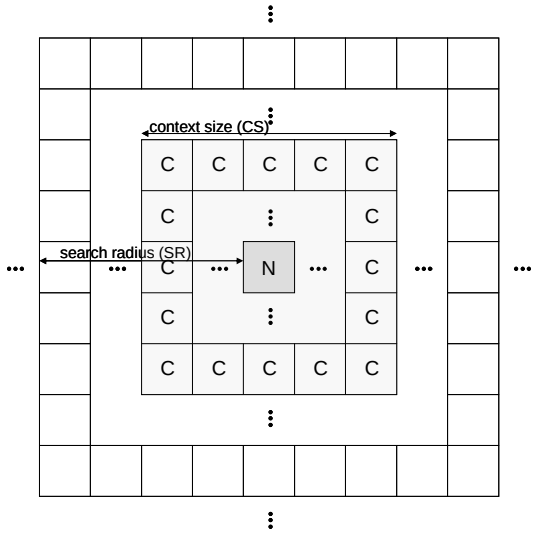

Figure 1. The CBPF proposed for image denoising

The algorithm which replaces a noisy pixel through the presented context-based prediction technique is described in the following pseudocode:

```
CBP (x, y, SR, CS, T)
      For i:=x-SR to x+SR, 0≤i<W
            For j:=y-SR to y+SR, 0≤j<H
                  If i=x AND j=y then
                        Continue
                  If SAD(x, y, i, j, CS)<T AND NOT Salt_Pepper(i, j) then
                        Q[Color(i, j)]:=Q[Color(i, j)]+1
      Return Max(Q)
```

The parameters of the *CBP* function are: the position of the current pixel, the search area defined by *SR*, *CS* which gives the order of the model and the similarity threshold *T*. Obviously, the noisy pixel is not part of the context. In order to improve the algorithm efficiency, we do not search for identical contexts; we accept similar contexts, measuring the similarity degree as the sum of absolute differences:

$$SAD = \sum_{j=0}^{CS-1}\sum_{i=0}^{CS-1}\left|B_1(i,j) - B_2(i,j)\right|, \text{ without } i = j = \frac{CS}{2} \tag{6}$$

The following pseudocode presents how we compute the sum of absolute differences:

```
SAD (x1, y1, x2, y2, CS)
      S:=0
      For i:= -CS/2 to CS/2, 0≤i+x1<W, 0≤i+x2<W, do
            For j:= -CS/2 to CS/2, 0≤j+y1<H, 0≤j+y2<H do
                  If i=0 AND j=0 then
                        Continue
                  S:=S + |Color(i+x1, j+y1)-Color(i+x2, j+y2)|
      Return S
```

Since the noisy pixel is not part of the context, the value of the middle pixel must be avoided in the *SAD* computation. We have considered a context similar if the *SAD* value is less than a certain threshold *T*. We keep in *Q* how many times a certain pixel value has occurred after the considered pixel. The *Max* function returns the color (index) of the highest element from *Q*. The noise-free pixel value occurred in similar contexts with the highest frequency will replace the noisy pixel value *N*. If there is at least one valid case, it is returned by the *CBP* function. If similar contexts have not been found, the initial noisy pixel is unchanged, but this case is very rare. We have checked if a pixel is noisy with the *Salt_Pepper* function returning TRUE for pixels having values of 0 or 255. The *CBPF* algorithm is presented in the following pseudocode:

```
CBPF(CS, SR, T)
      For i:=0 to W-1 do
            For j:=0 to H-1 do
                  If Salt_Pepper(i, j) then
                        Set_Color(i, j, CBP(i, j, CS, SR, T))
```

where the *Set_Color* function replaces the value of the noisy pixel (*i*, *j*) with the value returned by the *CBP* function.

4. Experimental Methodology

We have implemented our CBPF algorithm in C#, whereas the implementations of the state-of-the-art denoising methods used for comparisons were available in Matlab. The tests were performed on three 512×512 grayscale PNG images: Boat, Cameraman and Airplane. We have added salt-and-pepper noise into the original images, in ratios between 10% and 90%, in steps of 10%. All the methods were compared using this set of noisy images.

The performances of the denoising methods were expressed in terms of *MSE* and *PSNR*. The *MSE* shows the error values of a filtered image *F* compared with the original one *O*:

$$MSE = \frac{\sum_{i=0}^{W-1}\sum_{j=0}^{H-1}\left(F(i,j)-O(i,j)\right)^2}{n \cdot m} \tag{7}$$

where *W* and *H* are the width and height of the image, respectively. On the other hand, the *PSNR* estimates the quality of a denoised image with respect to the original one. The *PSNR* is computed as follows:

$$PSNR = 10 \cdot \log_{10} \frac{255^2}{MSE} \tag{8}$$

The goal is to obtain a low *MSE* and a high *PSNR*.

5. Experimental Results

First, we have evaluated the CBPF by varying *CS* on a fixed *SR*=5 and *T*=500. As we have explained in Section 3, the *CS* can have only odd values and it must be at least 3. The *MSE* values obtained on the test images are presented in Figure 2.

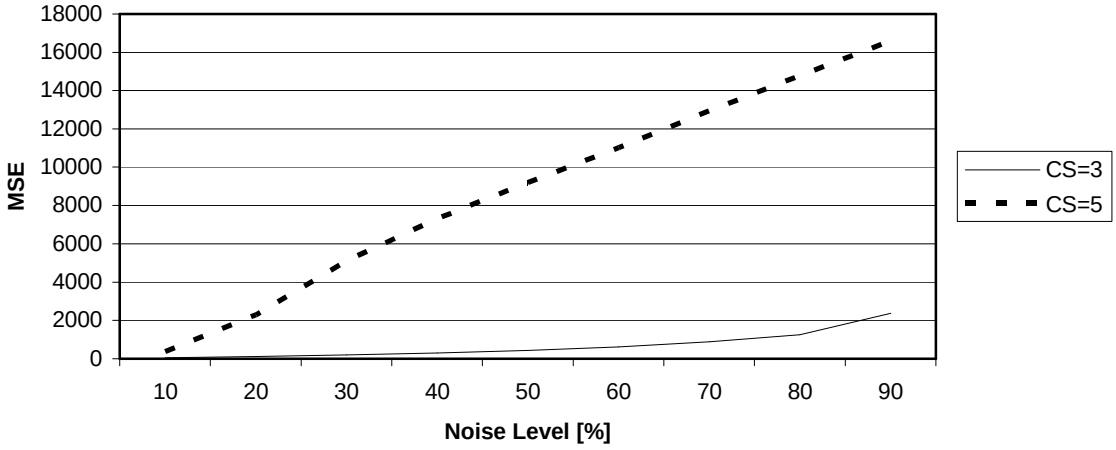

a.

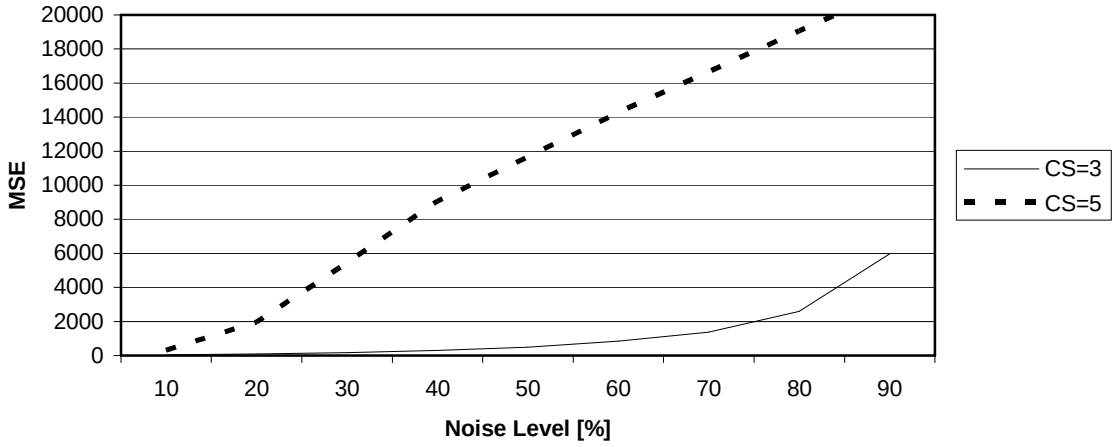

b.

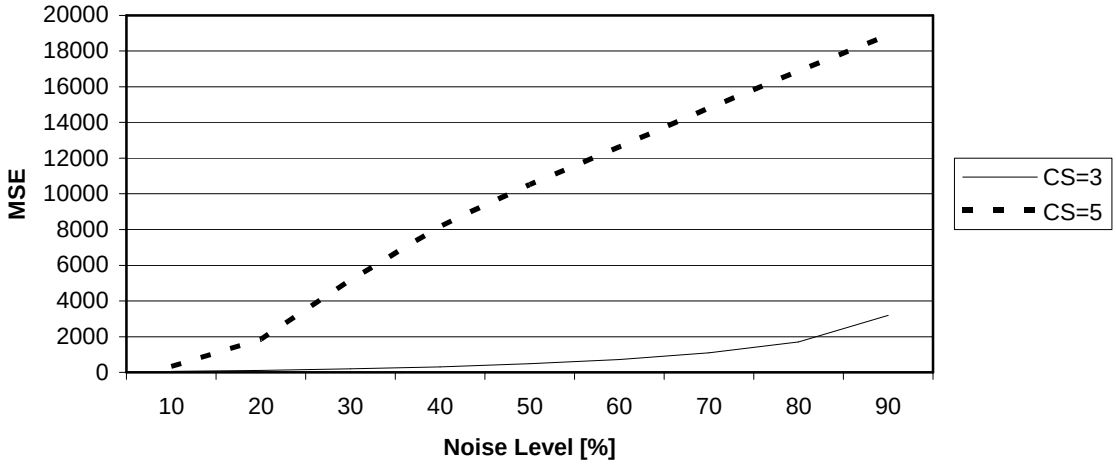

c.

Figure 2. The MSE of the Boat **(a)**, Cameraman **(b)** and Airplane **(c)** images denoised using CBPF with different context sizes

Figure 2 has shown that the best value for *CS* is 3, the CBPF being inefficient for higher contexts. A richer context leads to higher precision, but if it is too rich, the probability to find it is low. Therefore, usually the performance is increasing together with the context up to a certain size (which in our application is 3), after which it starts to decrease.

We have continued our evaluations by varying the search radius *SR* between 2 and 5, considering the best *CS*=3 and a fixed *T*=500. The *MSE* values obtained on the test images are presented in Figure 3.

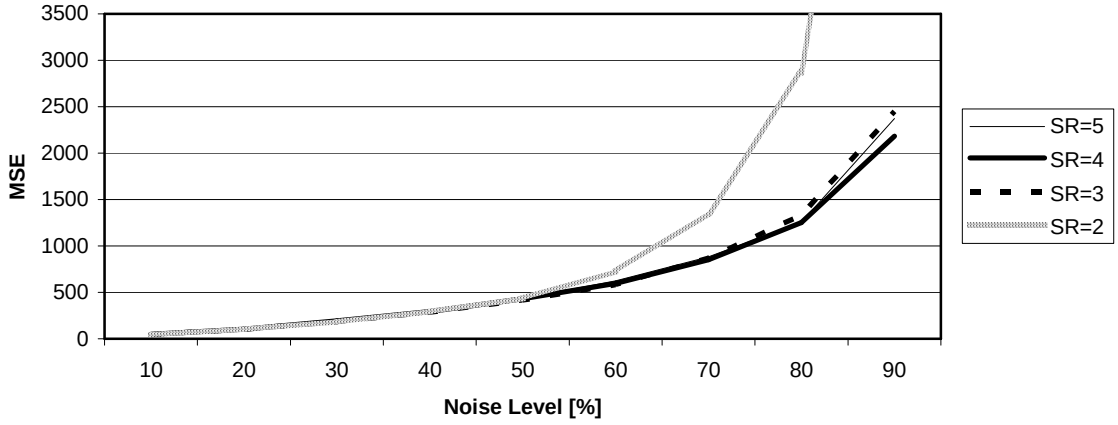

a.

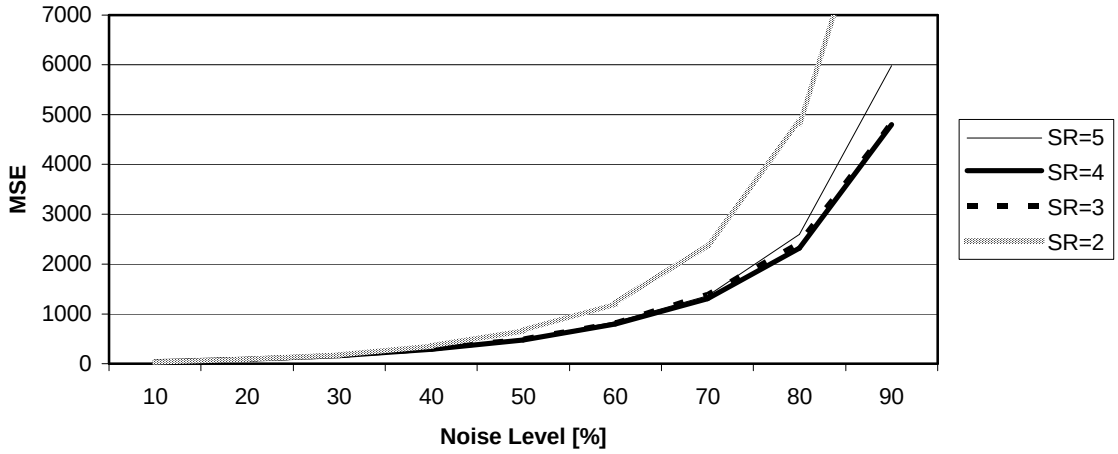

b.

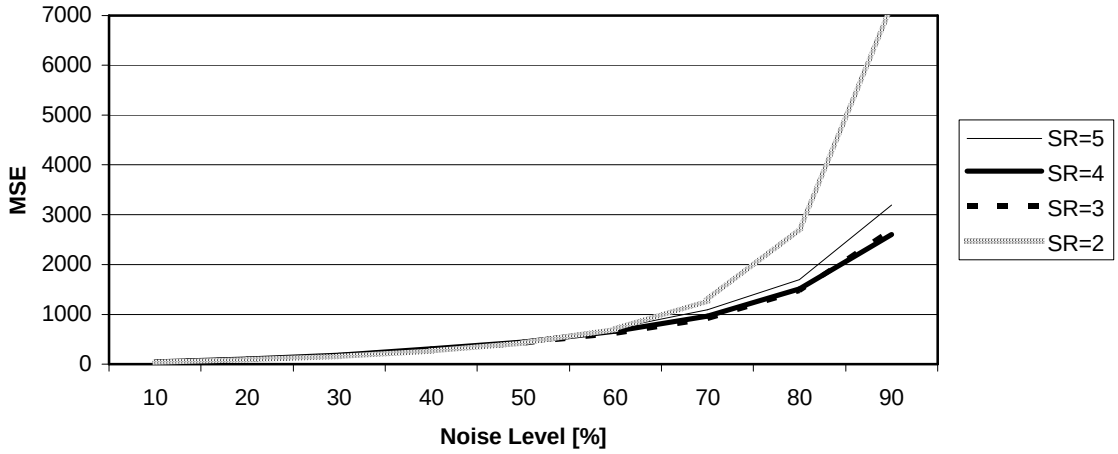

c.

Figure 3. The MSE of the Boat **(a)**, Cameraman **(b)** and Airplane **(c)** images denoised using CBPF with different search radius values

One can observe that on the Boat image, a CBPF with *SR* value of 3 is better up to 60% noise level and for *SR* of 4 is better only starting with 70% noise density. On the Airplane image the *SR* of 2 is better up to 50%, while *SR* of 3 and 4 are very close and better starting with a noise of 60%. On the Cameraman image *SR* 4 performs best, it being just slightly outperformed by *SR* 2 on a noise up to 20%. Therefore, we consider that the optimal SR value will be 4. The conclusion after this evaluation step was that the search area might be sufficiently high to find the context, but if it is too high ($SR \geq 5$), the multiple pixel value choices can lead to uncertainty and thus to lower denoising ability.

The next stage of our analysis consists in varying the similarity threshold *T* between 450 and 600, in steps of 50. As we have already explained, when we have searched for the context of the current noisy pixel, we have taken into account all the contexts whose similarity degree, computed as SAD, is less than *T*. Figure 4 presents the *MSE* obtained for different similarity threshold values, considering the best $CS=3$ and the optimal $SR=4$.

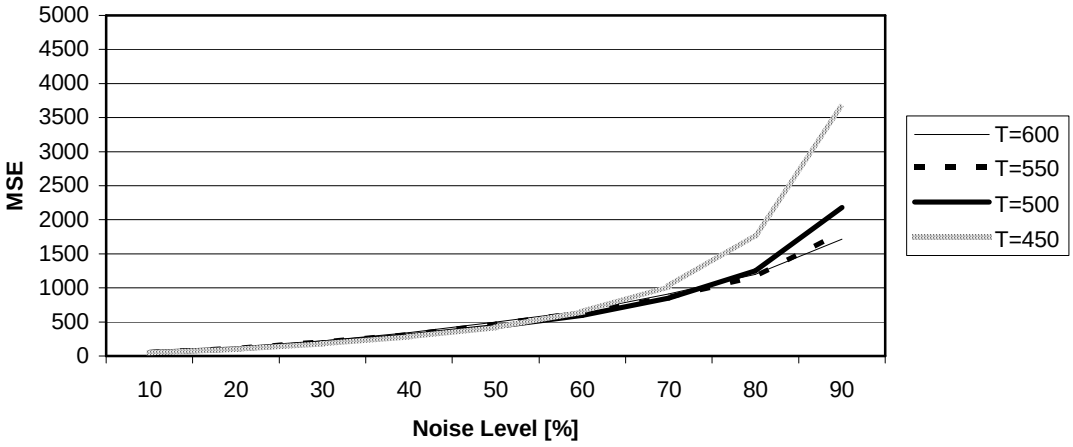

a.

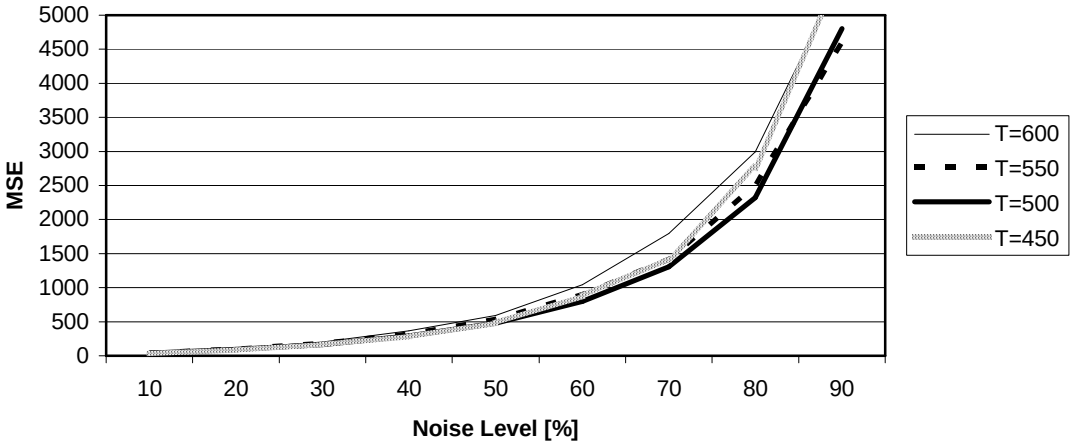

b.

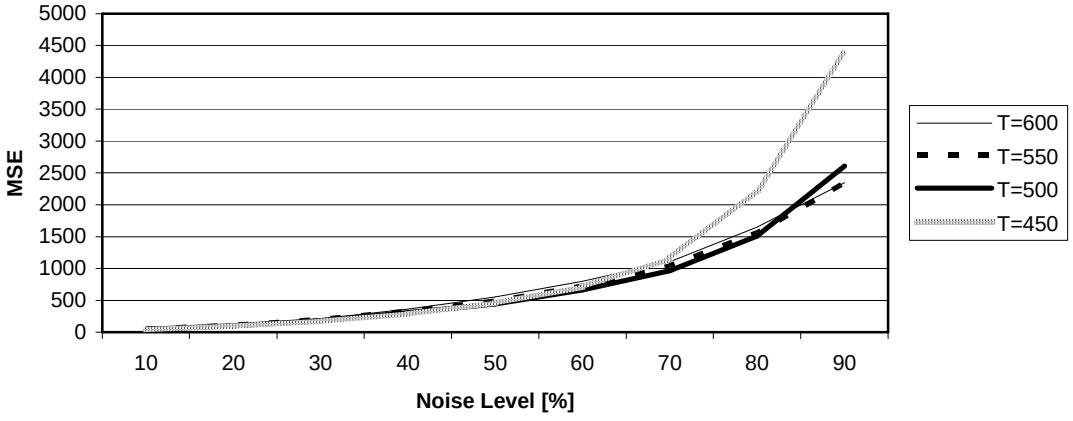

c.

Figure 4. The *MSE* of the Boat **(a)**, Cameraman **(b)** and Airplane **(c)** images denoised using CBPF with different search similarity thresholds

Figure 4 showed that the best similarity threshold value is 500 up to 70% noise on the Boat image and even up to 80% noise on the Cameraman and Airplane images. Only on very high noise density, a threshold of 550 or 600 is slightly better. Therefore, we have considered that the optimal similarity threshold value will be *T*=500. A difference of 500 in the *SAD* between two compared image blocks, taking into account the best *CS*=3 (contexts of 8 pixels), results in a reasonable average per pixel difference of 62.

Further, we have compared the optimal CBPF having *SR*=4, *CS*=3 and *T*=500 with other denoising methods. We have included in the comparative analysis the Noise Adaptive Fuzzy Switching Median Filter (NAFSMF) [13], the Decision Based Algorithm (DBA) [4], the Median Filter (MF), the Progressive Switching Median Filter (PSMF) [8], the Relaxed Median Filter (RMF) [7] and the Analysis Prior Algorithm (APA) [37]. Figures 5 and 6 present comparatively the *MSE* and *PSNR*, respectively, for all the considered methods, including our CBPF with *SR*=4, *CS*=3 and *T*=500, on the Boat, Cameraman and Airplane test images.

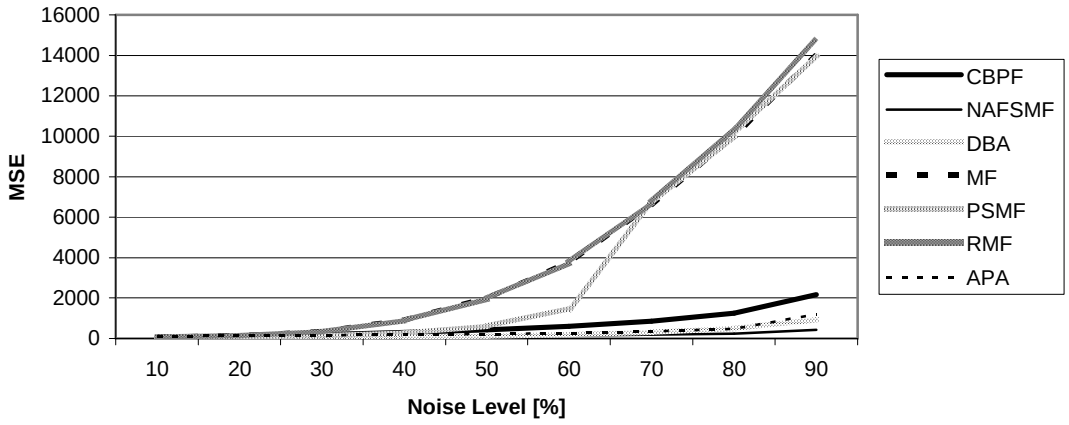

a.

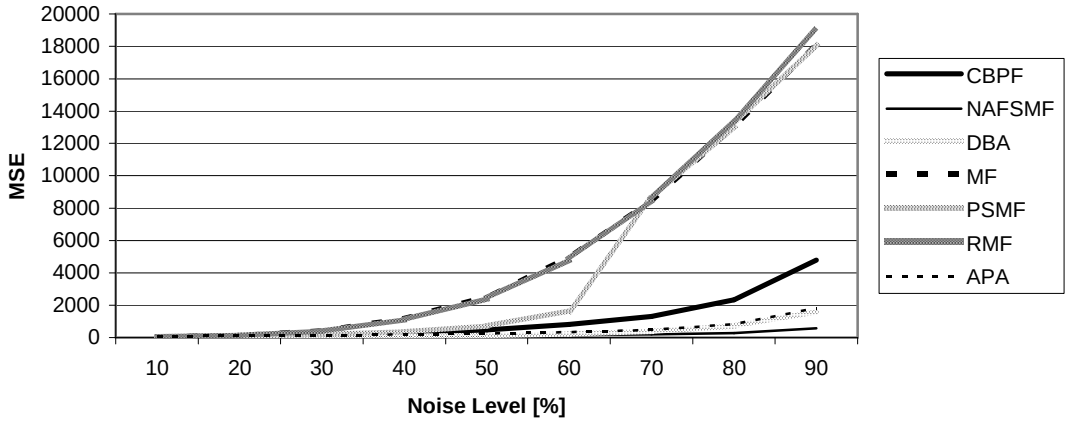

b.

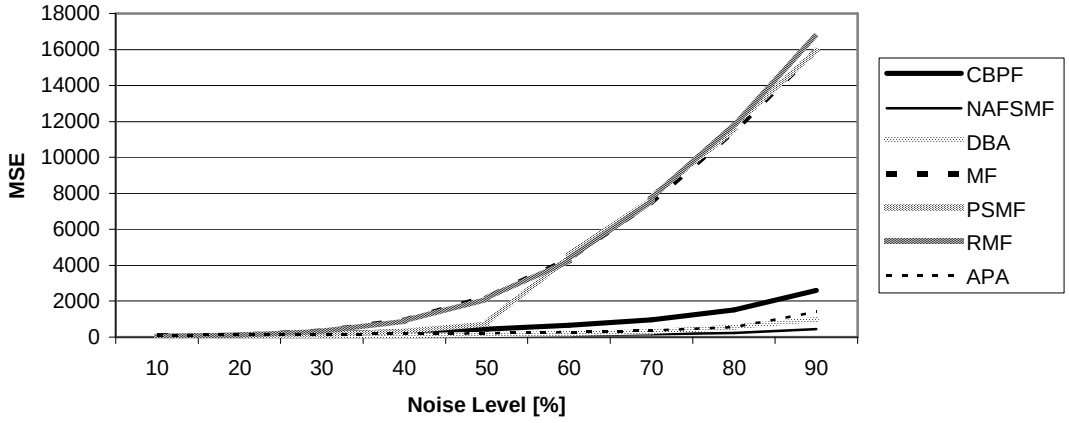

c.

Figure 5. Comparing the MSE on the Boat **(a)**, Cameraman **(b)** and Airplane **(c)** images

The *MSE* and *PSNR* results show that the CBPF outperforms the MF, PSMF and RMF denoising methods. It also partially outperformed the APA method, on noise levels up to 20%. It is less performing than the NAFSMF and DBA methods.

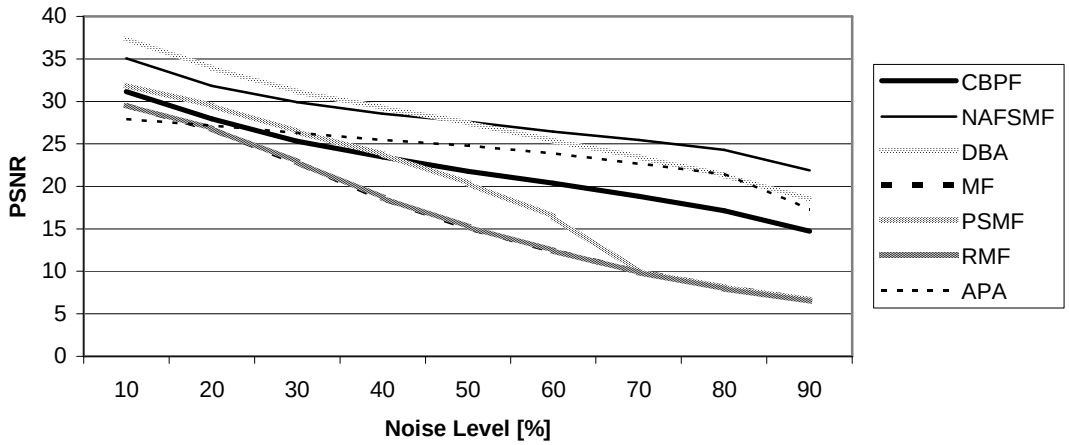

a.

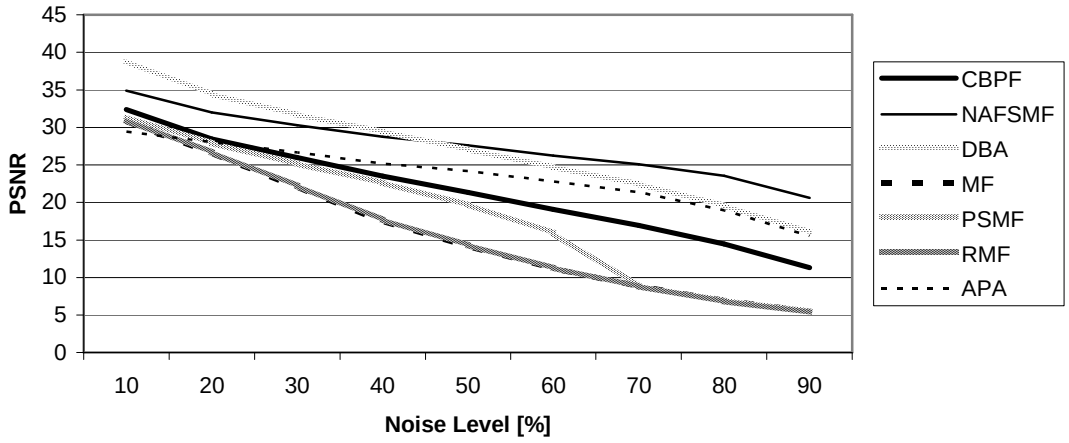

b.

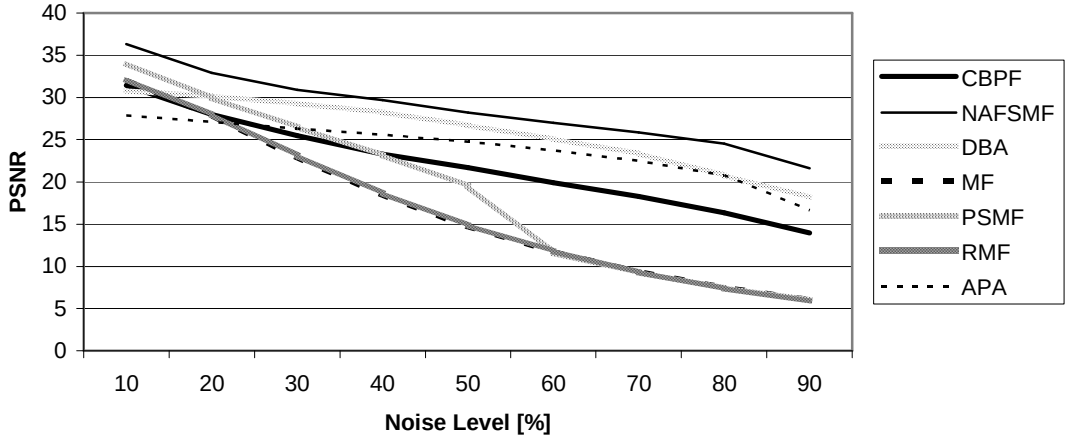

c.

Figure 6. Comparing the PSNR on the Boat **(a)**, Cameraman **(b)** and Airplane **(c)** images

Figure 7 presents the Cameraman image with 30% salt-and-pepper noise (a) and its denoised versions using our CBPF (b), as well as using NAFSM (c), DBA (d), MF (e), PSMF (f), RMF (g), APA (h).

a.

b.

c.

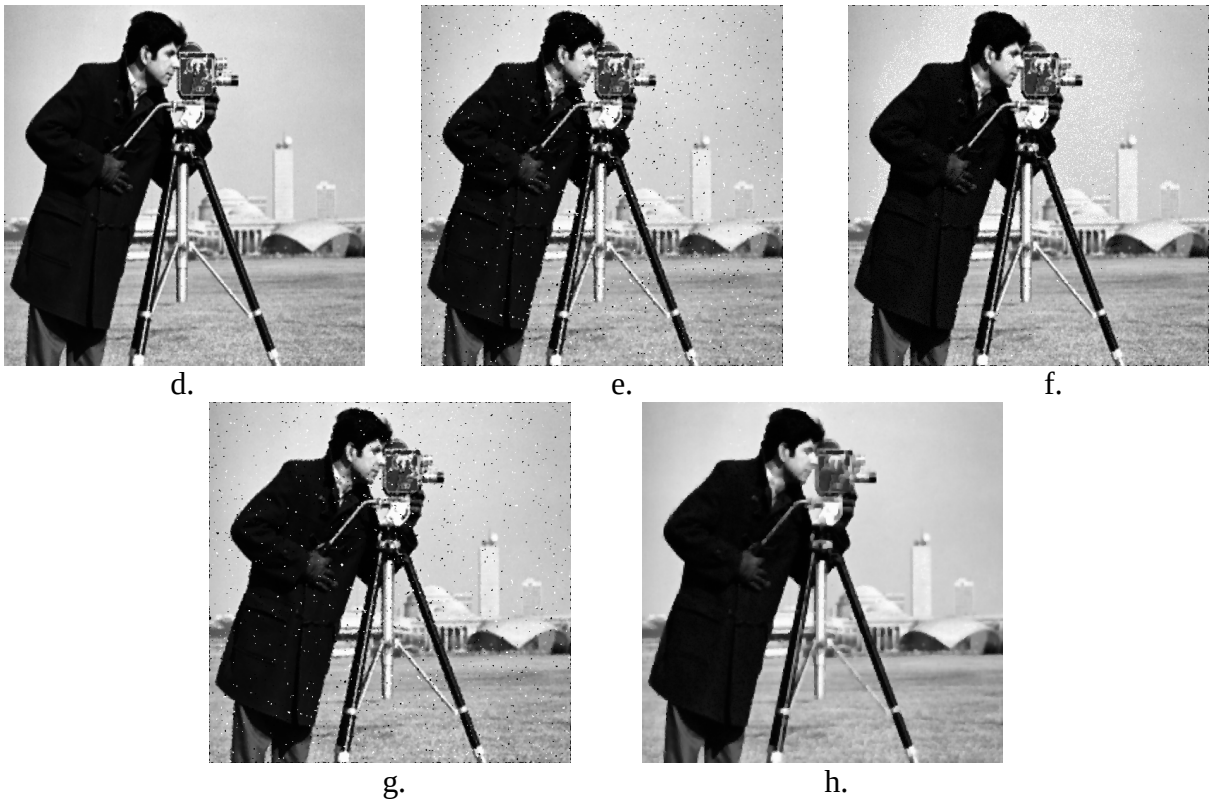

Figure 7. Denoising the Cameraman image with 30% noise **(a)** using the CBPF **(b)**, NAFSM **(c)**, DBA **(d)**, MF **(e)**, PSMF **(f)**, RMF **(g)**, APA **(h)**

As Figure 7 depicts, the proposed CBPF can better remove salt-and-pepper noise than the MF, PSMF and RMF denoising methods.

6. Conclusions and Further Work

In this paper, we have proposed a new filtering method for impulse noise on grayscale images using context-based prediction. The CBPF replaces a pixel affected by salt-and-pepper noise with the pixel which occurred in its neighborhood, determined by the search radius input parameter, with the highest frequency in the same context as the replaceable pixel. The frequencies of pixels occurring in a certain context are determined like in a Markov chain. Since our method is using context information, it can reconstruct details in the images affected by noise better than other methods. Due to the intrinsic behavior, it could have a significant advantage on images containing textures. The limitation of the proposed method stands in the computational time required for denoising, which recommends it only for off-line processing of images.

We have analyzed our CBPF by varying its parameters. The tests performed on the Boat, Cameraman and Airplane images show that the CBPF with a context size of 3 is the optimal. In the next step, we have shown that the optimal search radius is 4. The last analyzed parameter was the similarity threshold whose optimal value was 500, admitting reasonable differences between the compared image blocks. We have compared the optimal CBPF (with configuration *CS*=3, *SR*=4, *T*=500) with other existing denoising methods in terms of *MSE* and *PSNR*. The experimental results show that the CBPF significantly outperforms the MF, the PSMF and also the RMF and it is not significantly worse than the NAFSMF and the DBA

methods (see Figures 5 and 6). It also partially outperforms, on low noise levels, other considered algorithms. For the case of usual noise filtering conditions (noise between 0-30%), the proposed method is very close to the most performing denoising methods referenced. Therefore, in our opinion, this new method can be further developed, so that it could outperform all the existing methods. It is a new method, which is using context information, and has a high further development potential.

Although the optimal *SR* is 4, there are some noise levels where a *SR* of 3, or even 2, is better. Therefore, as a further work direction, we will analyze the possibility to dynamically adjust the *SR* value and thus to adapt this input parameter to the image. Other possible further work directions are the dynamic context size adaptation, the use of other context shapes, the run-time computation of the similarity threshold based on the context size, as well as the use of the CBPF in a hybrid system together with fuzzy and neural methods.

Acknowledgments

We express our gratitude to Jeno-Sorin Gyorfi for providing his useful and competent help in evaluating all the denoising methods used for comparisons with our CBPF.

References

[1] Dong, Y., Chan, R.H., Xu, S.: 'A Detection Statistic for Random-Valued Impulse Noise', IEEE Transactions on Omage Processing, 16, (4), 2007, pp. 1112-1120.

[2] Bhatia, A., Kulkarni, R.K.: 'Removal of High Density Salt-And-Pepper Noise Through Improved Adaptive Median Filter', International Conference on Computer Science and Information Technology, Bangalore, May 2012, pp. 197-200.

[3] Lal, S., Kumar, S., Chandra, M.: 'Removal of High Density Salt & Pepper Noise Through Super Mean Filter for Natural Images', International Journal of Computer Science Issues, 9, (3), May 2012, pp. 303-309.

[4] Srinivasan, K.S., Ebenezer, D.: 'A New Fast and Efficient Decision Based Algorithm for Removal of High Density Impulse Noise', IEEE Signal Processing Letters, 14, (3), 2007, pp. 189-192.

[5] Esakkirajan, S., Veerakumar, T., Subramanyam, A.N., PremChand, C.H.: Removal of High Density Saltand Pepper Noise Through Modified Decision Based Unsymmetric Trimmed Median Filter', IEEE Signal Processing Letters, 18, (5), May 2011, pp. 287-290.

[6] Lu, C.T., Chou, T.C.: 'Denoising of Salt-and-Pepper Noise Corrupted Image using Modified Directional-Weighted-Median Filter', Pattern Recognition Letters, 33, (10), July 2012, pp. 1287-1295.

[7] Hamza, A.B., Luque-Escamilla, P., Martínez-Aroza, J., Román-Roldán, R.: 'Removing Noise and Preserving Details with Relaxed Median Filters', Journal of Mathematical Imaging and Vision, 11, (2), October 1999, pp. 161-177.

[8] Wang, Z., Zhang, D.: 'Progressive Switching Median Filter for the Removal of Impulse Noise from Highly Corrupted Images', IEEE Transactions on Circuits and Systems II: Analog and Digital Signal Processing, 46, (1), January 1999, pp. 78-80.

[9] Wang, G., Li, D., Pan, W., Zang, Z.: 'Modified Switching Median Filter for Impulse Noise Removal', Signal Processing, 90, (12), December 2010, pp. 3213-3218.

[10] Lukac, R., Plataniotis, K.N., Venetsanopoulos, A.N.: 'A Statistically-Switched Adaptive Vector Median Filter', Journal of Intelligent and Robotic Systems, 42, (4), April 2005, pp. 361-391.
[11] Duan, D., Mo, Q., Wan, Y., Han, Z.: 'A Detail Preserving Filter for Impulse Noise Removal', International Conference on Computer Application and System Modeling, Taiyuan, China, October 2010, pp. 265-268.
[12] Jassim, F.A.: 'Kriging Interpolation Filter to Reduce High Density Salt and Pepper Noise', World of Computer Science and Information Technology Journal, 3, (1), 2013, pp. 8-14.
[13] Toh, K.K.V., Isa, N.A.M.: 'Noise Adaptive Fuzzy Switching Median Filter for Salt-and-Pepper Noise Reduction', IEEE Signal Processing Letters, 17, (3), March 2010, pp. 281-284.
[14] Lin, T.C.: 'SVM-based Filter Using Evidence Theory and Neural Network for Image Denoising', Journal of Software Engineering and Applications, 6, (3B), pp. 106-110, 2013, pp. 106-110.
[15] Deng, C., Liu, H.M., Wang, Z.H.: 'Applying an Improved Neural Network to Impulse Noise Removal', International Conference on Wavelet Analysis and Pattern Recognition, Qingdao, China, July 2010, pp. 207-210.
[16] Aizenberg, I., Wallace, G.: 'Intelligent Detection of Impulse Noise using Multilayer Neural Network with Multi-Valued Neurons', Image Processing: Algorithms and Systems X and Parallel Processing for Imaging Applications II, February 2012, p. 82950S.
[17] Soares, P.L.B., Silva, J.P.: 'Neural Networks Applied for Impulse Noise Reduction from Digital Images', INFOCOMP Journal of Computer Science, 11, (3-4), 2012, pp. 7-14.
[18] Türkmen, I.: 'Removing Random-Valued Impulse Noise in Images Using Neural Network Detector', Turkish Journal of Electrical Engineering and Computer Science, 22, (3), 2014, pp. 637-649.
[19] Mishra, S.K., Panda, G., Meher, S.: 'Chebyshev Functional Link Artificial Neural Networks for Denosing of Image Corrupted by Salt and Pepper Noise', ACEEE International Journal on Signal and Image Processing, 1, (1), January 2010, pp. 42-46.
[20] Agostinelli, F., Anderson, M.R., Lee, H.: 'Adaptive Multi-Column Deep Neural Networks with Application to Robust Image Denosing', Advances in Neural Information Processing Systems 26, Lake Tahoe, Nevada, USA, December 2013, pp. 1493-1501.
[21] Xie, J., Xu, L., Chen, E.: 'Image Denoising and Inpainting with Deep Neural Networks', Advances in Neural Information Processing Systems 25, Lake Tahoe, Nevada, USA, December 2012, pp. 350-358.
[22] Nair, M.S., Shankar, V.: 'Predictive-Based Adaptive Switching Median Filter for Impulse Noise Removal using Neural Network-Based Noise Detector', Signal and Video Processing, 7, (6), November 2013, pp. 1041-1070.
[23] Surrah, H.A.: 'Impulse Noise Removal from Highly Corrupted Images using new Hybrid Technique based on Neural Networks and Switching Filters', Journal of Global Research in Computer Science, 5, (3), 2014, pp. 1-7.
[24] Chen, S., Shi, W., Zhang, W.: 'An Efficient Universal Noise Removal Algorithm Combining Spatial Gradient and Impulse Statistic', Mathematical Problems in Engineering, 2013, p. 480274
[25] Zeng, X., Yang, L.: 'Mixed Impulse and Gaussian Noise Removal using Detail-Preserving Regularization', Optical Egineering, 49, (9), September 2010, p. 097002.
[26] Buades, A., Coll, B., Morel, J.-M.: 'A Non-Local Algorithm for Image Denosing', IEEE Computer Society Conference on Computer Vision and Pattern Recognition, Vol. 2, San Diego, CA, USA, June 2005, pp. 60-65.

[27] Estrada, F., Fleet, D., Jepson, A.: 'Stochastic Image Denoising', British Machine Vision Conference, London, September 2009, p. 117.
[28] Wong, A., Mishra, A., Zhang, W., Fieguth, P., Clausi, D.A.: 'Stochastic Image Denoising Based on Markov-Chain Monte Carlo Sampling', Signal Processing, 91, (8), 2011, pp. 2112-2120.
[29] Jääskinen, V., Parkkinen, V., Cheng, L., Corander, J.: 'Bayesian clustering of DNA sequences using Markov chains and a stochastic partition model', Statistical Applications in Genetics and Molecular Biology, 13, (1), February 2014, pp. 105-121.
[30] Marques, A., Belo, O.: 'Discovering Student web Usage Profiles Using Markov Chains', The Electronic Journal of e-Learning, 9, (1), 2011, pp. 63-74.
[31] Gambs, S., Killijian, M.O., del Prado Cortez, M.N.: 'Next Place Prediction using Mobility Markov Chains', Proceedings of the First Workshop on Measurement, Privacy, and Mobility, New York, USA, April 2012, p. 3.
[32] Cao, G., Nie, J.-Y., Bai, J.: 'Using Markov Chains to Exploit Word Relationships in Information Retrieval', The 8th Conference on Large-Scale Semantic Access to Content, Pittsburgh, Pennsylvania, USA, 2007, pp. 388-402.
[33] Mushtaq, A., Lee, C.-H.: 'An Integrated Approach to Feature Compensation Combining Particle Filters and Hidden Markov Model for Robust Speech Recognition', IEEE International Conference on Acoustics, Speech, and Signal Processing, Kyoto, Japan, March 2012, pp. 4757-4760.
[34] Gellert, A., Florea, A., Vintan, M., Egan, C., Vintan, L:, 'Unbiased Branches: An Open Problem', Twelfth Asia-Pacific Computer Systems Architecture Conference, Seoul, Korea, August 2007, pp. 16-27.
[35] Rabiner, L.R.: 'A Tutorial on Hidden Markov Models and Selected Applications in Speech Recognition', Proceedings of the IEEE, 77, (2), 1989, pp. 257-286.
[36] Gellert, A., Florea, A.: 'Web Page Prediction Enhanced with Confidence Mechanism', Journal of Web Engineering, 13, (5-6), USA, November 2014, pp. 507-524.
[37] Majumdar, A., Ward, R.K.: 'Synthesis and Analysis Prior Algorithms for Joint-Sparse Recovery', IEEE International Conference on Acoustics, Speech and Signal Processing, March 2012, pp. 3421-3424.